Heliyon 10 (2024) e21943

Contents lists available at ScienceDirect

Heliyon

journal homepage: www.cell.com/heliyon

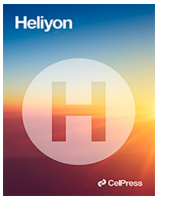

Recovery of ergosterol from *Agaricus bisporus* mushrooms via supercritical fluid extraction: A response surface methodology optimisation

Cláudia F. Almeida [a,b,c], Yaidelin A. Manrique [a,c,*], José Carlos B. Lopes [a,c], Fernando G. Martins [b,c], Madalena M. Dias [a,c]

[a] *LSRE-LCM – Laboratory of Separation and Reaction Engineering – Laboratory of Catalysis and Materials, Faculty of Engineering, University of Porto, Rua Dr. Roberto Frias, 4200-465 Porto, Portugal*

[b] *LEPABE – Laboratory for Process Engineering, Environment, Biotechnology and Energy, Faculty of Engineering, University of Porto, Rua Dr. Roberto Frias, 4200-465 Porto, Portugal*

[c] *ALiCE – Associate Laboratory in Chemical Engineering, Faculty of Engineering, University of Porto, Rua Dr. Roberto Frias, 4200-465 Porto, Portugal*

A R T I C L E I N F O

Keywords:
Agaricus bisporus mushroom
Supercritical fluid extraction
Response surface methodology
Ergosterol
Carbon dioxide

A B S T R A C T

This work uses the response surface methodology to optimise ergosterol recovery from *Agaricus bisporus* mushrooms by supercritical fluid extraction. The influence of pressure, temperature, co-solvent use, and solvent-to-mushroom mass ratio was evaluated on yield and extract composition. Considering temperature, pressure, and co-solvent volume percentage, predictive models were regressed for extraction yield, ergosterol purity in the recovered fractions, and ergosterol recovery. The co-solvent volumetric fraction was the most influential factor, increasing the extraction yield and reducing the extract's ergosterol purity. A maximum ergosterol extract purity of (547.27 ± 2.37) $mg_{ergosterol} \cdot g_{extract}^{-1}$ was obtained at a pressure of 100 bar, temperature of 50 °C and co-solvent volume percentage of 5 % v/v. The highest ergosterol recovery was (6.23 ± 0.06) $mg_{ergosterol} \cdot g_{dw}^{-1}$ for operating conditions of 244 bar, 56 °C, and 8 % v/v of co-solvent. Coefficients of determination close to one were obtained for all models, indicating good agreement with experimental data.

1. Introduction

The food industry generates large amounts of residues that must be treated, minimised, or eliminated, promoting a circular economy. Mushroom harvesting, in particular, produces waste reaching up to 20–30 % of the production volume, commonly used in low-economic-value animal feed and compost [1]. Furthermore, predictions indicate an increase in the mushroom world production from 14.35 million tons in 2020 to 24.05 million tons by 2028, thus causing a yearly excess residue between 1.9 and 2.9 million tons by 2028 [2]. In addition, most by-products consist of discarded bases or stripes that, although difficult to process, contain substantial amounts of high-added-value substances [1,3]. Thus, a valorisation chain for these residues is a necessity, with several studies

* Corresponding author. LSRE-LCM – Laboratory of Separation and Reaction Engineering – Laboratory of Catalysis and Materials, Faculty of Engineering, University of Porto, Rua Dr. Roberto Frias, 4200-465 Porto, Portugal.
E-mail address: yaidelin.manrique@fe.up.pt (Y.A. Manrique).

https://doi.org/10.1016/j.heliyon.2023.e21943
Received 1 September 2023; Received in revised form 31 October 2023; Accepted 31 October 2023
Available online 7 November 2023

reporting the mushrooms' chemical composition, extraction methodologies or functionalisation of extracted fractions [4–12]. **Table S1** (Supplementary data) summarises publications concerning the extraction of added-value molecules from different mushroom species, indicating the targeted compounds, extraction methodologies and main results. Polysaccharides, phenols, and sterols are the most recurring target compounds found in mushroom extracts, as shown in **Table S1** (Supplementary data). Other works explore the extraction of fatty acids; peptides, amino acids and proteins; flavonoids and anthocyanins; carbohydrates; pigments; and eritadenine. In fact, most mushroom species present high mycosterols content, and ergosterol (5,7,22-ergostatrien-3β-ol) is generally the most abundant [13,14]. This compound and its derivatives are known for a wide range of health-related properties, such as antioxidant, antityrosinase, antitumor, antimicrobial, and anti-inflammatory activities [15–18]. It also has a powerful antihyperlipidemic action, reducing cholesterol levels similarly to phytosterols [15,19,20]. Furthermore, vitamin D_2, also known as ergocalciferol, can be obtained through ultraviolet (UV) treatment of ergosterol molecules [16,21]. This added-value nutrient is recommended for consumption by the European Food Safety Authority (EFSA) as it is involved in calcium and phosphorus absorption and, consequently, impacts bone mineralisation [22]. Despite containing small amounts of vitamin D_2, mushrooms are rich in ergosterol (circa 90 % of its sterol fraction), thus envisaging the sustainable production of vitamin D_2 via UV radiation [14,23,24]. Studies by Mattila et al. [25] evaluated sterols and vitamin D_2 content in species of wild (*Chantarellus cibarius, C. tubaeformis, Botelus edulis* and *Lactarius trivialis*) and cultivated mushrooms (*Pleurotus ostreatus, Agaricus bisporus*/brown, *Agaricus bisporus*/white and *Lentinus edodes*). The authors reported a higher ergosterol content in cultivated mushrooms (6.02–6.79 mg/g dw) than in wild mushrooms (2.96–4.89 mg/g dw); whereas vitamin D_2 showed an inverse tendency, being almost absent in cultivated mushrooms and having higher concentrations in wild mushrooms (4.7–194 μg/100 g dw). Due to the aforementioned reasons, ergosterol is the target compound of this work.

Frequently studied mushroom species (see Supplementary data, **Table S1**) include *Agaricus bisporus* (button), *Lentinula edodes* (shiitake), and *Pleurotus ostreatus* (oyster), which are also the most consumed globally [2,26]. Of the over 12 000 mushroom species currently identified, circa 2000 are considered edible, but only about 20 are industrially cultivated, processed and commercialised [27,28]. Of these, *Agaricus bisporus* contributed 61.8 % to the 2021 global mushroom market in terms of volume [26]. Barreira, Oliveira [13] quantified ergosterol content in seven wild (*Amanita caesarea*, *B. edulis*, *C. cibarius*, *Fistulina hepatica*, *Lactarius deliciosus*, *Macrolepiota procera*, and *Morchella esculenta*) and six cultivated (*Agaricus bisporus*, *Agaricus bisporus Portobello*, *Flammulina velutipes*, *L. edodes*, *Pleurotus eryngii*, and *P. ostreatus*) mushroom species, determining the highest ergosterol content (3.52 mg/g dw) in *Agaricus bisporus*. Thus, this abundant mushroom species was the targeted in this work.

Table S1 (Supplementary data) also compiles a variety of extraction methodologies, among which the most common are solvent or Soxhlet extraction. These conventional techniques frequently include high solvent consumption, expensive and often toxic solvents, time-consuming procedures with high energy requirements (mainly due to long-term heating), and low extraction yields and/or lack of selectivity regarding the targeted compounds [29]. Thus, there has been an increased interest towards emerging green technologies that bridge these weaknesses, which include microwave-assisted extraction (MAE), ultrasound-assisted extraction (UAE), supercritical fluid extraction (SFE), pressurised liquid extraction (PLE), pulsed electric field (PEF) extraction, and enzyme-assisted extraction (EAE) [8,30,31]. In particular, supercritical fluid extraction with carbon dioxide (SFE-CO_2) has several advantages, including: low cost, non-combustible, non-toxic and non-explosive solvent; preservation of the extracted fractions' properties, such as flavour and aroma; products not contaminated with solvents; and the potential for selective and fractional extraction of compounds [32,33]. Carbon dioxide is adequate for dissolving lipophilic compounds due to its nil dipole moment; however, its lack of polarity makes it unsuitable for extracting polar substances [30,31]. The workaround solution consists of adding a polar modifier or co-solvent (e.g., water, methanol, ethanol, acetic acid or ethylene glycol), which increases the solubility towards polar compounds at the compromise of the obtained extracts' purity [31]. For instance, Gil-Ramírez et al. [34] report a higher selectivity regarding sterol content in the *Agaricus*

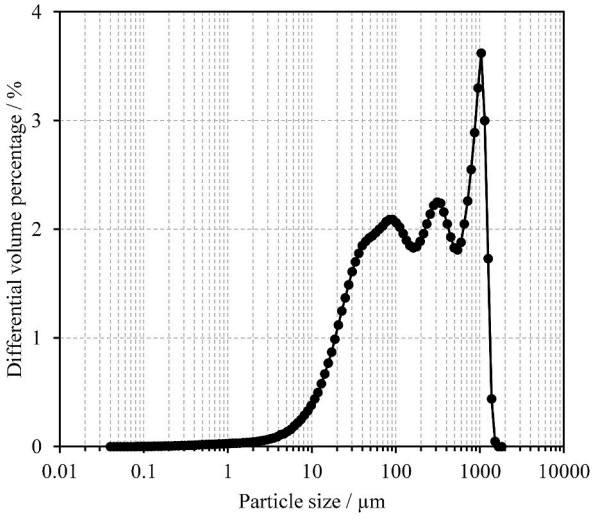

Fig. 1. Volumetric particle size distribution for the fresh *Agaricus bisporus* mushroom powder.

bisporus fractions obtained with pure supercritical carbon dioxide compared to those obtained with the addition of 10 % ethanol as co-solvent (approximately 50 % versus 30 %); nevertheless, adding co-solvent results in higher extraction yields (2 % versus 0.5 %). Supercritical fluid extraction with carbon dioxide is explored in the current work; adding ethanol as a co-solvent is also addressed.

This work aims to optimise ergosterol recovery from *Agaricus bisporus* mushrooms obtained via supercritical fluid extraction with carbon dioxide. Proper design of experiments (DoE), such as central composite design (CCD) or Box Behnken design (BBD), allows for a reduction in the number of experimental tests [35]. In this work, experiments were performed using a three-factor CCD considering temperature, pressure, and co-solvent volume percentage. RSM was used to regress three predictive models for overall extraction yield, ergosterol recovery per mushroom dry weight, and ergosterol purity on the recovered fractions. The effect of the solvent-to-mushroom mass ratio is also studied. Furthermore, Soxhlet extractions are performed, with ethanol and *n*-hexane, for comparative purposes with raw materials from other works and with the recovered SFE fractions.

This work reports the quantitative dependence of ergosterol extraction from *Agaricus bisporus* mushrooms via supercritical fluid extraction, uniquely including the comprehensive study of the effect of pressure, temperature and co-solvent volume percentage, and also providing a model to calculate the extraction yield as well as ergosterol recovery and purity in the extract.

2. Materials and methods

2.1. Raw material

Agaricus bisporus white mushrooms were purchased from a local supermarket in March 2022. All samples were weighted, lyophilised (in a VirTis benchtop K Freeze-Dryer for 48 h, at 40 mTorr and −80 °C), and reduced to a powder using a blender. Fig. 1 shows the corresponding volume-based particle size distribution obtained by Laser Diffraction Particle Size Analyser (Beckman Coulter, LS230 model). The moisture content was determined at (92.37 ± 0.26) % w/w from the mass difference before and after the freeze-drying process. The powder was wrapped in aluminium foil for light-protection and stored in a zip lock bag at 4 °C until further use.

2.2. Standards and reagents

Pressurised bottled carbon dioxide (CE number 204-696-9, >99.998 %) was supplied by Air Liquide. Absolute ethanol (CAS 64-17-5) and *n*-hexane (CAS 110-54-3, 95 %, HPLC grade) were obtained from VWR chemicals. The analytical standards of cholesterol (CAS 57-88-5, >99 %), ergosterol (CAS 57-87-4, ≥ 75 %) and palmitic acid (CAS 57-10-3, ≥ 99 %) were purchased from Sigma-Aldrich. The linoleic acid standard (CAS 60-33-3, >97 %) was acquired from TCI chemicals.

2.3. Extraction methodologies

2.3.1. Soxhlet extraction

Soxhlet extractions, with *n*-hexane and ethanol, were performed in dehydrated a mushroom sample (approximately 4 g) for 4 h. The collected fractions were dried in a vacuum rotary evaporator at 40 °C and the dried content was measured to calculate the extraction yield

$$Y_{\text{ext}}(\%) = \frac{m_{\text{extract}}(\text{g})}{m_{\text{dry mushroom}}(\text{g})} \times 100 \tag{1}$$

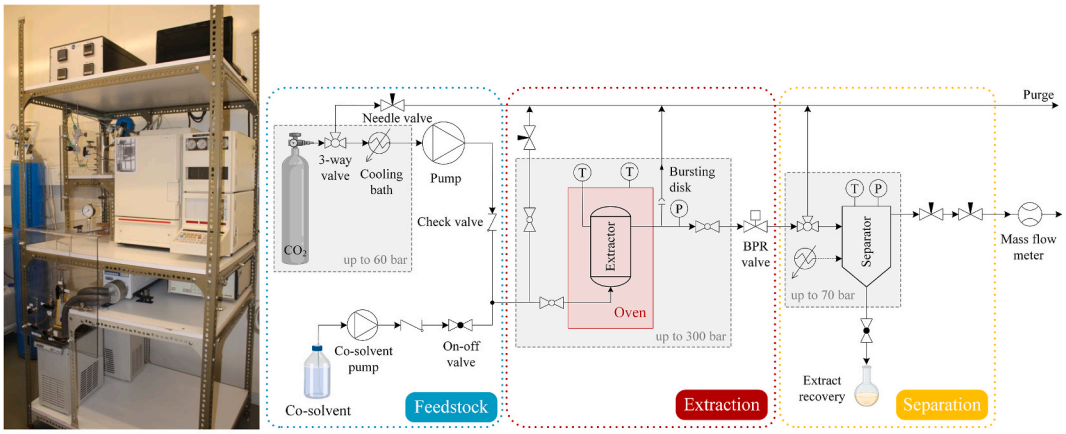

Fig. 2. Supercritical fluid extraction (SFE) equipment: (A) photograph, and (B) schematic representation.

i.e., the ratio between the mass of extract, $m_{extract}$, and the mass of dry mushroom sample, $m_{dry\ mushroom}$. Extracts were stored at 4 °C until further analysis.

2.3.2. Supercritical fluid extraction (SFE)

An existing bench-scale SFE-CO_2 equipment (Fig. 2) was used to extract *Agaricus bisporus* samples. The setup includes an extraction vessel and a separator with maximum working pressures of 300 and 70 bar, respectively. Both vessels are made of stainless steel, allowing temperatures up to 80 °C. Mushroom powder samples mixed with glass beads were placed in a basket (internal dimensions: 30 mm diameter and 130 mm height), and then in the extraction cell. Solvent-to-mushroom ratio, extraction temperature, pressure and co-solvent volume percentage were studied to determine optimum extraction conditions. The equipment was operated continuously in all experiments, with a constant total flow rate of 4 mL/min (including carbon dioxide and co-solvent). The temperature inside the separator never exceeded 20 °C, and the extracted compounds precipitated in this vessel due to the imposed pressure drop by the back pressure regulator (BPR) valve, that controls the pressure in the extractor vessel according to a predefined set-point value. Recovered fractions were dried in a rotary vacuum evaporator at 40 °C, and the respective dry matter content was measured to calculate the extraction yield according to **Equation (1)**. Extracts were stored in the cold, at 4 °C, until further analysis. At the end of the extraction process, a cleaning procedure was performed by feeding absolute ethanol from the extractor's outlet tube into the separator, thus allowing the drag and recovery of all remaining extract.

2.4. GC-MS analysis

Agaricus bisporus extracts (1 g/L) were analysed using a GC-MS TQ8040 NX Triple Quadrupole from Shimadzu (Japan), equipped with an automatic injector (AOC-20i) and a cross-bonded fused low-polarity silica column (Rxi-5Sil MS, Restek, USA) of 30 m length, 0.25 mm ID and 0.25 μm film thickness. Injection temperature and pressure were set to 260 °C and 100 kPa, respectively. Ion source and interface temperatures were defined as 220 and 300 °C, respectively. Oven temperature was programmed for 60 °C during the first minute, then increased to 300 °C at the rate of 10 °C/min and held for 15 min. A sample volume of 1 μL was injected for each analysis, and the helium flow rate was set at 1.61 mL/min. The mass scanning range was defined from m/z 40 to 500, and the ionisation voltage was 70 V. The compounds were identified by comparing the obtained mass spectra with those of the database from the National Institute of Standards and Technology (library NIST 147). Ergosterol and fatty acids (linoleic and palmitic) analytical standards were used to determine the calibration curves for quantifying the extracts. Cholesterol at a concentration of 0.1 g/L was added to all samples as an internal standard (IS). All analyses were performed in duplicates, with results reported as mean ± standard deviation (SD).

2.5. Response surface methodology

2.5.1. Experimental design

SFE experimental planning was performed according to a three-factor central composite design considering pressure (P, bar), temperature (T, °C) and co-solvent volume percentage (f, % v/v). **Table S2** (Supplementary data) shows the experimental domain of the inscribed central composite design, including the coded and natural values. The following expression allows the conversion between these variables

$$x_n = x_{n,av} + \frac{\Delta x_n}{\Delta x_c} x_c \tag{2}$$

where x_n and x_c are the natural and coded values of the independent variables. Δx_n and Δx_c represent the difference between the maximum and minimum values for the factors' natural and coded values; $x_{n,av}$ is the average value of the natural independent variable considering the range of analysis.

As shown in **Table S2** (Supplementary data), experimental points include five levels for each variable distributed around the central point of a sphere, which was repeated thrice to increase the model's precision. Experimental design in these conditions resulted in 17 experiments, which were randomly performed to reduce the impact of random errors on the results. The distance from the central point, α, was set to the default value of 1.6818.

2.5.2. Mathematic model

TIBCO Statistica® (version 14.0.0.15) was used for experimental design planning and data treatment, including response surface modelling with a fit of the experimental data to a second-order polynomial model

$$Y = \beta_0 + \sum_{i=1}^{k} \beta_j x_i + \sum_{i=1}^{k} \beta_{ii} x_i^2 + \sum_{i=1}^{k-1} \sum_{j>i}^{k} \beta_{ij} x_i x_j \tag{3}$$

where Y is the model's predicted response (dependent variable), and x_i and x_j are the factors' coded values (i.e., the independent coded variables). β_0, β_i, β_{ii}, and β_{ij} are the regression coefficients for the intercept, linear, quadratic and interaction terms, respectively, and k represents the number of factors ($k = 3$, in this study).

Three response (dependent) variables were studied: the overall extraction yield (Y_{ext}), given by **Equation (1)**; the ergosterol recovery (R_{erg}), that is the amount of ergosterol extracted per mass of dry mushroom sample; and the ergosterol purity on the recovered

fractions (P_{erg}), that is the amount of ergosterol per mass of extract.

The three response variables are related according to

$$R_{erg}\left(mg_{ergosterol} \cdot g_{dw}^{-1}\right) = \frac{P_{erg}\left(mg_{ergosterol} \cdot g_{extract}^{-1}\right) Y_{ext}(\%)}{100} \quad (4)$$

2.5.3. Statistical analysis

Statistical calculations were performed using the TIBCO Statistica® (version 14.0.0.15) software. Analysis of Variance (ANOVA), coefficients of determination (i.e., R-squared and adjusted R-squared) and lack-of-fit tests evaluated the regressed models' suitability. Statistically significant terms for each response variable of **Equation (3)** were identified using Tukey tests with a confidence level of 95% (i.e., a significance level of $\alpha = 0.05$). Non-significant coefficients were discarded, thus simplifying the models. The models' consistency to describe experimental data was evaluated by comparison of observed and model-predicted values. An analysis of the residuals was also performed to further validate the models.

3. Results and discussion

3.1. Soxhlet extraction

Soxhlet extractions were performed in dehydrated mushroom samples with *n*-hexane and ethanol as solvents. **Table 1** summarises the extractions' main results, including the type of solvent used, extraction time (t), number of cycles per extraction, extraction yield (Y_{ext}), ergosterol purity on the recovered fractions (P_{erg}) and its recovery per mushroom dry weight (R_{erg}).

Analysing **Table 1**, ethanol extractions resulted in a higher Y_{ext}, higher R_{erg} and a lower P_{erg} when compared with *n*-hexane extractions, in accordance with previous results by Heleno, Diz [14]. The *n*-hexane extractions align with those performed by Barreira, Oliveira [13] regarding ergosterol recovery per mushroom's DW, $R_{erg} = (3.52 \pm 0.01)\ mg_{ergosterol} \cdot g_{dw}^{-1}$. Heleno, Diz [14] achieved a lower recovery, $R_{erg} = (1.861 \pm 0.003)\ mg_{ergosterol} \cdot g_{dw}^{-1}$, attributing the difference to the mushrooms' cultivation conditions and related secondary metabolites production. For ethanol extractions, results concerning the extract purity in ergosterol were comparable with those of Heleno, Diz [14], with P_{erg} values of circa 56 $mg_{ergosterol} \cdot g_{extract}^{-1}$. However, lower extraction yields were obtained in this work (9.6 versus 12.0 %), which consequently translates into lower ergosterol recovery (5.44 versus 6.76 $mg_{ergosterol} \cdot g_{dw}^{-1}$). This discrepancy may be related to the higher number of extraction cycles in this work, causing a lower solid/solvent contact time per cycle and thus hindering extraction.

Supercritical fluid extraction results should follow the tendencies identified above. Ethanol as a polarity modifier is projected to increase Y_{ext} and R_{erg} at the compromise of lowering the extract's purity in ergosterol. Contrarily, pure supercritical carbon dioxide extractions are comparable with *n*-hexane extractions, as both solvents are apolar. In these cases, a more refined fraction (i.e., a higher P_{erg}) of ergosterol is expected at the trade-off of lower Y_{ext} and ergosterol recovery per mushroom dry weight.

3.2. Supercritical fluid extraction

3.2.1. Solvent-to-mushroom ratio optimisation

Preliminary extractions of *Agaricus bisporus* mushrooms were performed using supercritical carbon dioxide (CO_2) as the main solvent and ethanol as a polarity modifier. Considering the experimental domain presented in **Table S2** (Supplementary data), preliminary tests have shown that both the extraction yield (Y_{ext}) and the ergosterol recovery per mushroom dry weight (R_{erg}) are maximised at the following conditions: pressure of 244 bar, temperature of 56 °C; and co-solvent percentage of 8 % v/v. Thus, these experimental conditions were fixed to evaluate the solvent-to-mushroom ratio (S/M) effect on the response variables. S/M accounts for both carbon dioxide and ethanol. Fig. 3 and **Table S3** (Supplementary data) show the experimental results of Y_{ext}, P_{erg}, and R_{erg} for distinct S/M ratios. The values of P_{erg} and R_{erg} were not determined for the lowest studied ratio, $S/M = 64$, due to its low extraction yield. The extraction yield results in Fig. 3A show an increase from 0.45 % for an $S/M = 64$ to a fourfold increase for $S/M = 300$. For $S/M = 352$, Y_{ext} remains constant at approximately 2 % due to the raw material's exhaustion, meaning that all the extractable compounds (at the considered operational conditions) have been removed from the mushroom's matrix. The slightly lower Y_{ext} value (circa 1.87 %) observed for $S/M = 416$ is not significative, given that composition variations are expected in natural raw materials (depending on, for example, the mushroom body part and developmental stage) [34]. Considering the data up to the Y_{ext} plateau (i.e., excluding the last two points of **Table S3** from Supplementary data), Fig. 3A shows a linear dependence between Y_{ext} and S/M ratio, implying that the extraction's limiting step is the compounds' solubility in the solvent and not mass transfer limitations [36,37].

Fig. 3B (filled circles) shows an increase in ergosterol recovery for S/M ratios up to 300; from this value forward, a plateau is

Table 1
Soxhlet extraction yields and ergosterol composition.

Solvent	t/h	Number of cycles	Y_{ext}/%	$P_{erg}/mg_{ergosterol} \cdot g_{extract}^{-1}$	$R_{erg}/mg_{ergosterol} \cdot g_{dw}^{-1}$
n-Hexane	4	25	1.81	238.32 ± 12.64	3.65 ± 0.19
Ethanol		28	9.57	56.83 ± 0.36	5.44 ± 0.03

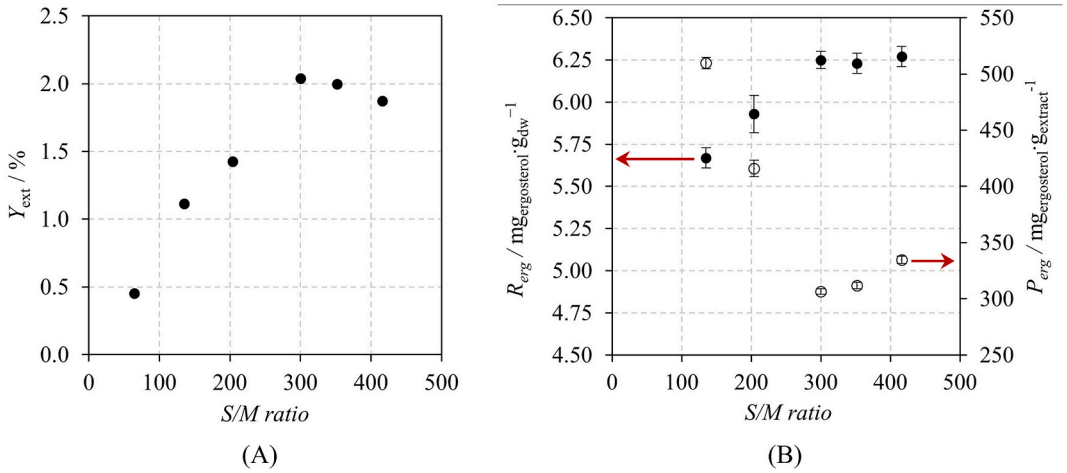

Fig. 3. Effect of the solvent-to-mushroom mass ratio on the (A) supercritical fluid extraction yield, and (B) ergosterol content (unfilled circles) and recovery per mushroom's dry weight (filled circles). Extractions were performed by varying the S/M ratio with the following operating conditions: pressure of 244 bar, temperature of 56 °C and 8 % v · v^{-1} co-solvent (ethanol).

reached at approximately 6.2 $mg_{ergosterol} \cdot g_{dw}^{-1}$. Heleno, Diz [14] obtained a similar ergosterol recovery using ultrasound-assisted extraction for 15 min at 375 W. Moreover, a similar dependence on the solvent-to-mushroom ratio is observed by comparing Fig. 3A and B, meaning that the increase in the extraction yield is reflected in the additional extraction of ergosterol. Contrarily, the ergosterol purity in the extract displays an inverse tendency, decreasing for increasing *S/M* ratios; this response stabilises at circa 300 $mg_{ergosterol} \cdot g_{extract}^{-1}$ for an $S/M \geq 300$. This result shows that higher extraction yields, obtained at higher *S/M* ratios, resulted not only from additional ergosterol but also from other compounds' recovery. Thus, ergosterol content in the extracted fractions is lower when a higher *S/M* ratio is used. A slightly higher P_{erg} and lower Y_{ext} were obtained for an *S/M* ratio of 416. Given that these responses are proportional to the ergosterol recovery (**Equation (4)**), the value of R_{erg} obtained is similar to other experimental points in the plateau. Therefore, the lower extraction yield is associated with lower recovery of compounds other than ergosterol, thus increasing this compound's purity in the extract.

An *S/M* ratio of 350 was fixed for further extractions, compromising the extracts' ergosterol purity but maximising the extraction yield and ergosterol recovery.

3.2.2. Response surface methodology

Supercritical fluid extractions were performed according to the experimental design described in Section 2.5.1, which resulted in

Table 2
Response surface methodology optimisation; coded and natural values for the factors' experimental domain and respective experimental (Obs) and model predicted (Pred) responses.

ID	Factor (dependent variable)			Response (independent variable)					
	P/bar (x_1)	T/°C (x_2)	f / % v · v^{-1} (x_3)	Y_{ext}/%		$P_{erg}/mg_{ergosterol} \cdot g_{extract}^{-1}$		$R_{erg}/mg_{ergosterol} \cdot g_{dw}^{-1}$	
				Obs	Pred	Obs	Pred	Obs	Pred
1	190 (0)	50 (0)	10 (+ α)	2.140	2.091	186.31 ± 8.80	188.53	3.99 ± 0.19	4.14
2	280 (+ α)	50 (0)	5 (0)	1.406	1.461	434.46 ± 11.83	462.69	6.11 ± 0.17	6.58
3	100 (− α)	50 (0)	5 (0)	1.090	1.117	547.27 ± 2.37	516.57	5.97 ± 0.03	5.89
4 (CP)	190 (0)	50 (0)	5 (0)	1.524	1.515	300.70 ± 6.67	309.34	4.58 ± 0.10	4.67
5	190 (0)	40 (− α)	5 (0)	1.499	1.512	395.35 ± 6.39	389.38	5.93 ± 0.10	6.06
6	136 (−1)	56 (+1)	2 (−1)	1.223	1.128	424.48 ± 9.68	435.73	5.19 ± 0.12	4.82
7	136 (−1)	44 (−1)	2 (−1)	1.137	1.110	529.25 ± 4.24	547.42	6.02 ± 0.05	6.30
8 (CP)	190 (0)	50 (0)	5 (0)	1.502	1.515	318.55 ± 2.42	309.34	4.78 ± 0.04	4.67
9	190 (0)	50 (0)	0 (− α)	0.834	0.965	462.78 ± 4.12	458.09	3.86 ± 0.03	4.10
10	244 (+1)	56 (+1)	8 (+1)	1.999	1.968	311.80 ± 2.96	295.37	6.23 ± 0.06	5.68
11 (CP)	190 (0)	50 (0)	5 (0)	1.534	1.515	308.34 ± 5.28	309.34	4.73 ± 0.08	4.67
12	136 (−1)	44 (−1)	8 (+1)	1.347	1.351	427.29 ± 13.75	439.61	5.76 ± 0.19	5.49
13	244 (+1)	56 (+1)	2 (−1)	0.931	0.869	518.69 ± 14.99	508.11	4.83 ± 0.14	4.83
14	244 (+1)	44 (−1)	8 (+1)	1.982	2.019	312.66 ± 8.59	303.15	6.20 ± 0.17	6.29
15	190 (0)	60 (+ α)	5 (0)	1.415	1.484	285.49 ± 8.57	288.99	4.04 ± 0.12	4.30
16	244 (+1)	44 (−1)	2 (−1)	1.370	1.287	393.17 ± 1.63	383.63	5.39 ± 0.02	4.85
17	136 (−1)	56 (+1)	8 (+1)	1.709	1.735	184.37 ± 3.14	195.66	3.15 ± 0.05	3.42

17 tests with three repetitions of the central point (CP). Table 2 displays the experiments' operational conditions using coded and natural values for the three factors (P, T, and f), and the main results obtained for each response (Y_{ext}, P_{erg}, and R_{erg}). Both the experimental (obs) and model prediction (pred) response variables are shown in Table 2. Table S4 (Supplementary data) shows the major fatty acids' composition (linoleic and palmitic acids) in each recovered SFE fraction. In both tables, P_{erg} and R_{erg} are given as mean ± SD, calculated from the duplicated GC-MS analyses performed on each extracted fraction. Other minor fatty acids reported in the literature [38,39] (e.g. myristic (C14:0), pentadecanoic (C15:0) and stearic (C18:0) acids) were also identified in some SFE fractions; however, these compounds were not quantified. As an example, Fig. 4 shows a GC-MS chromatogram from SFE extracts obtained from *Agaricus bisporus* mushrooms at a pressure of 190 bar, temperature of 50 °C and 10 % v · v^{-1} co-solvent, which resulted in the highest extraction yield (see Table 2).

Comparing experiments 1, 9 and the central points (4, 8, and 11) of Table 2, where pressure and temperature were fixed (P = 190 bar, T = 50 °C) and the co-solvent volume fraction was changed, a higher co-solvent volume percentage results in higher Y_{ext} and lower P_{erg}. This outcome was previously predicted in Section 3.1 and is corroborated by comparing experiments 10 with 13, 7 with 12, 6 with 17, and 4 with 16. The influence of the co-solvent volume percentage in ergosterol recovery is not as straightforward and requires a more detailed analysis. Similarly, the impacts of pressure and temperature on the Y_{ext}, P_{erg} and R_{erg} are not linear. Both cases are studied below.

Table S4 (Supplementary data) shows that the linoleic acid's extract purity ranges from 93.17 to 303.46 $mg_{linoleic\ acid} \cdot g^{-1}_{extract}$, with its recovery varying from 1.40 to 4.55 $mg_{linoleic\ acid} \cdot g^{-1}_{dw}$ depending on the extraction conditions. Palmitic acid is less abundant and has an extract purity between 48.78 and 73.35 $mg_{palmitic\ acid} \cdot g^{-1}_{extract}$ and recovery of 0.49–1.33 $mg_{palmitic\ acid} \cdot g^{-1}_{dw}$. The effects of pressure and temperature on the fatty acids' extract purity and recovery are complex and demand further analysis, which is not done in this work. Observing Table S4 (Supplementary data) and comparing experiments 1, 9 and the CPs (4, 8, and 11) for fixed pressure and temperature and different co-solvent volume percentages, higher f produce extracts with a lower content of fatty acids and a higher recovery. These effects are also validated by comparing experiments 10 with 13, 6 with 17, 7 with 12, and 14 with 16. The only exception is the linoleic acid recovery, which decreases with increasing ethanol volume percentage in experiments 6 and 17.

Table 3 shows the fitting coefficients for the interception, linear, quadratic, and interactive terms, along with the corresponding standard errors. This information is obtained by fitting the responses' experimental data, compiled in Table 2, to Equation (3)'s mathematic model. TIBCO's Software, Statistica® (version 14.0.0.15), was used to perform these regressions. Coefficients were deemed statistically non-significant (n.s.) within a 95 % confidence interval if their p-value was lower than 0.05; in these cases, the coefficient's value is not shown.

The coefficients shown in Table 3 validate previous conclusions. Namely, the influence of the co-solvent volume percentage on Y_{ext} is considered in the linear and interaction coefficients (β_3, β_{13} and β_{23}), being the quadratic effect non-significant within a 95 % confidence interval. All these coefficients are positive, thus validating an Y_{ext} increase for higher volumetric ethanol fractions. Contrarily, f's effect on P_{erg} is observed in the linear coefficient, β_3, and the interaction coefficient with temperature, β_{23}; both are negative, reinforcing ethanol's lowering impact on the ergosterol extract purity. As previously stated, ergosterol recovery shows a more elaborate dependence on ethanol's volumetric percentage, with two statistically relevant coefficients (β_{33} and β_{13}) of opposite signs. Closely examining the coefficients in Table 3 relating to Y_{ext}, f always has an increasing effect on the extraction yield. Furthermore, the temperature's influence is only statistically relevant in the interactive terms β_{12} and β_{23}, with opposing impacts. Concerning pressure, the following coefficients were observed: positive linear effect, statistically non-significant quadratic effect, positive interactive effect with f, and negative interactive effect with T. This last effect is directly related to carbon dioxide's density, whose higher values are expected to benefit extraction yields. The impact of pressure and temperature on carbon dioxide density

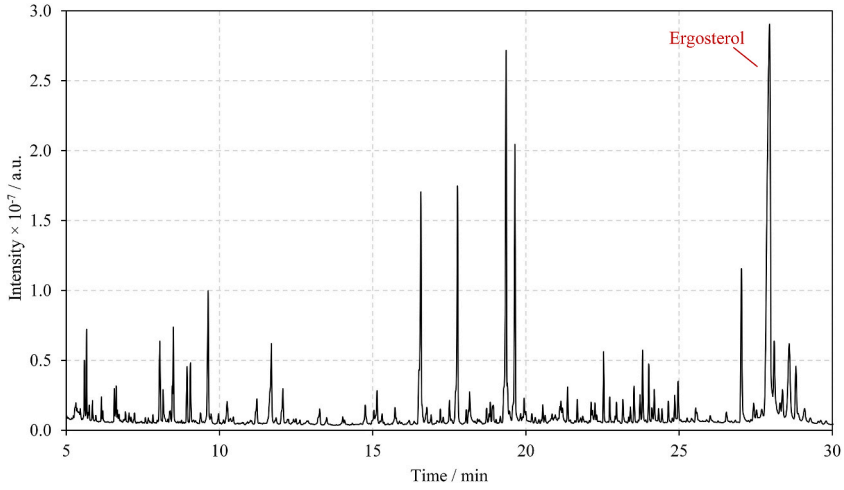

Fig. 4. GC-MS chromatogram of SFE extracts obtained from *Agaricus bisporus* mushrooms at a pressure of 190 bar, temperature of 50 °C and 10 % v/v co-solvent (ethanol).

Table 3
Fitting coefficients with the respective standard error for the three response variables studied.

Coefficient		Response (independent variable)		
		Y_{ext}/%	P_{erg}/ $mg_{ergosterol} \cdot g_{extract}^{-1}$	$R_{erg}/mg_{ergosterol} \cdot g_{dw}^{-1}$
Intercept	β_0	1.44 ± 0.06	326.27 ± 13.53	4.66 ± 0.19
Linear effect	β_1	0.39 ± 0.09	−135.62 ± 20.76	n.s.
	β_2	n.s.	−166.82 ± 24.03	−2.19 ± 0.33
	β_3	0.59 ± 0.06	−162.93 ± 14.27	n.s.
Quadratic effect	β_{11}	n.s.	289.26 ± 33.54	2.85 ± 0.46
	β_{22}	n.s.	n.s.	n.s.
	β_{33}	n.s.	n.s.	−0.54 ± 0.19
Interaction effect	β_{12}	−0.50 ± 0.16	252.95 ± 39.72	1.42 ± 0.55
	β_{13}	0.34 ± 0.10	n.s.	1.57 ± 0.32
	β_{23}	0.29 ± 0.12	−114.04 ± 29.30	n.s.

n.s.: statistically non-significant coefficient (p-value >0.05)

results in an overall lowering interactive effect on Y_{ext}. P_{erg} decreases with increasing ethanol volume percentages (β_3 and $\beta_{23} < 0$). Pressure displays a negative linear (β_1), positive quadratic (β_{11}), positive temperature-interactive (β_{12}), and non-significant f-interactive effect (β_{13}) on P_{erg}. Temperature has a lowering linear (β_2) and f-interactive (β_{23}) effect and an increasing pressure-interactive (β_{12}) effect on P_{erg}. Lastly, ergosterol recovery is enhanced at higher pressures for all cases (β_{11}, β_{12} and $\beta_{13} > 0$). Temperature displays a negative linear (β_2) and a positive pressure-interactive (β_{12}) impact on R_{erg}. Ethanol volumetric percentage decreases R_{erg} proportionally to its square ($\beta_{33} < 0$) and increases it proportionally to P and f ($\beta_{13} > 0$).

The regressed models, which can be used to predict Y_{ext}, P_{erg} and R_{erg}, are shown in Equations (5)–(7), respectively. In assembling these equations, statistically non-significant coefficients were discarded, and coded factors (x_i) were considered instead of natural values. Equation (2) can be used for conversion between both.

$$Y_{ext}(\%) = 1.44 + 0.39x_1 + 0.59x_3 - 0.50x_1x_2 + 0.34x_1x_3 + 0.29x_2x_3 \quad (5)$$

$$P_{erg}\left(mg_{ergosterol} \cdot g_{extract}^{-1}\right) = 326.27 - 135.62x_1 - 166.82x_2 - 162.93x_3 + 289.26x_1^2 + 252.95x_1x_2 - 114.02x_2x_3 \quad (6)$$

$$R_{erg}\left(mg_{ergosterol} \cdot g_{dw}^{-1}\right) = 4.66 - 2.19x_2 + 2.85x_1^2 - 0.54x_3^2 + 1.42x_1x_2 + 1.57x_1x_3 \quad (7)$$

Statistical information regarding the three regression models above is shown in Table 4, including coefficients of determination (R^2 and R^2_{adj}), ANOVA table summary and lack-of-fit test results.

The adjusted R-squared $\left(R^2_{adj}\right)$ values, shown in Table 4, are higher than 0.87 for all models, indicating an adequate selection of independent variables and excluding model overfitting. R-squared values (R^2), also shown in Table 4, are close to one for all regressed models, showing that the dependent variables' changes are well explained by the selected factors (independent variables). Coefficients with p-values higher than 0.05 are statistically non-significant and labelled with an asterisk. Other coefficients, with $p \leq 0.05$, directly influence the response variables and are displayed in Table 4.

The effect of the extraction conditions (P, T, and f) on the studied responses is graphically displayed by the contour plots in Fig. 5. These plots were obtained by fixing one factor at the domain's mid-value (see Supplementary data, Table S2). In this figure, blue dots indicate experimental data points and different z-axis' scales are used for better perceptibility. Fig. 5A shows that, at a fixed ethanol

Table 4
Coefficients of determination (R^2 and R^2_{adj}), lack-of-fit and ANOVA results for Y_{ext}, P_{erg} and R_{erg}.

Response variable		Y_{ext}			P_{erg}			R_{erg}		
Lack of fit/Mean square residual		0.0099			585.4			0.1105		
Coefficients of determination	R^2	0.9670			0.9787			0.9470		
	R^2_{adj}	0.9245			0.9513			0.8789		
Coefficient		**f**	**F-value**	**p**	**f**	**F-value**	**p**	**f**	**F-value**	**p**
Linear effect	β_1	1	21.2896	0.0024	1	42.6683	0.0003	1	0.6843	0.4354*
	β_2	1	0.8066	0.3990*	1	48.1960	0.0002	1	44.1131	0.0003
	β_3	1	101.8795	<0.0001	1	130.3775	<0.0001	1	2.6620	0.1468*
Quadratic effect	β_{11}	1	2.9742	0.1283*	1	74.3907	<0.0001	1	38.2618	0.0005
	β_{22}	1	0.0243	0.8805*	1	0.0886	0.7746*	1	0.9171	0.3701*
	β_{33}	1	0.3255	0.5862*	1	0.2129	0.6585*	1	7.7648	0.0270
Interaction effect	β_{12}	1	9.2478	0.0188	1	40.5579	0.0004	1	6.7782	0.0352
	β_{13}	1	12.7804	0.0090	1	0.7780	0.4070*	1	24.0982	0.0017
	β_{23}	1	5.8631	0.0460	1	15.1456	0.0060	1	2.1689	0.1843*

* indicates statistically non-significant coefficients (p-value >0.05).

percentage of 5 % v/v, higher Y_{ext} are obtained at higher pressures and lower temperatures, i.e., for increased carbon dioxide density. The lowest extraction yields occur at low pressures and temperatures. Fig. 5B displays an accentuated Y_{ext} increase for higher co-solvent volume percentages at a constant pressure of 190 bar. On the contrary, the temperature does not have such a pronounced effect. Fig. 5C shows a similar behaviour, with increasing Y_{ext} for higher f values; although having less impact, higher pressures also increase the Y_{ext}, mainly for higher ethanol volume percentages. Comparing the three previously mentioned plots, higher yields were obtained at higher pressures and co-solvent volume percentages. Also, f is the predominant factor (note the z-axis scales, which vary between plots). In Fig. 5D, a higher ergosterol purity in the recovered fractions is obtained at two ends of the pressure-temperature plane: lower pressure and temperature and higher pressure and temperature. Operating conditions in the PT plane's medium zone produce the least pure ergosterol extracts. Fig. 5E and F, regarding the extract's ergosterol purity, show the predominant effect of f over T and P, respectively. In both cases, lower co-solvent volume fractions result in purer ergosterol fractions. Fig. 5G shows a higher ergosterol recovery in the higher pressure region throughout the entire temperature range and at the lower temperatures and pressure points. Higher temperatures and low pressures result in lower R_{erg}. Fig. 5H shows that temperature's effect on ergosterol recovery has a greater influence on ergosterol recovery compared to ethanol volume percentage at a constant pressure. Furthermore, lower temperatures provide the highest ergosterol recovery for any f value. In contrast, increasing f for a fixed temperature does not significantly

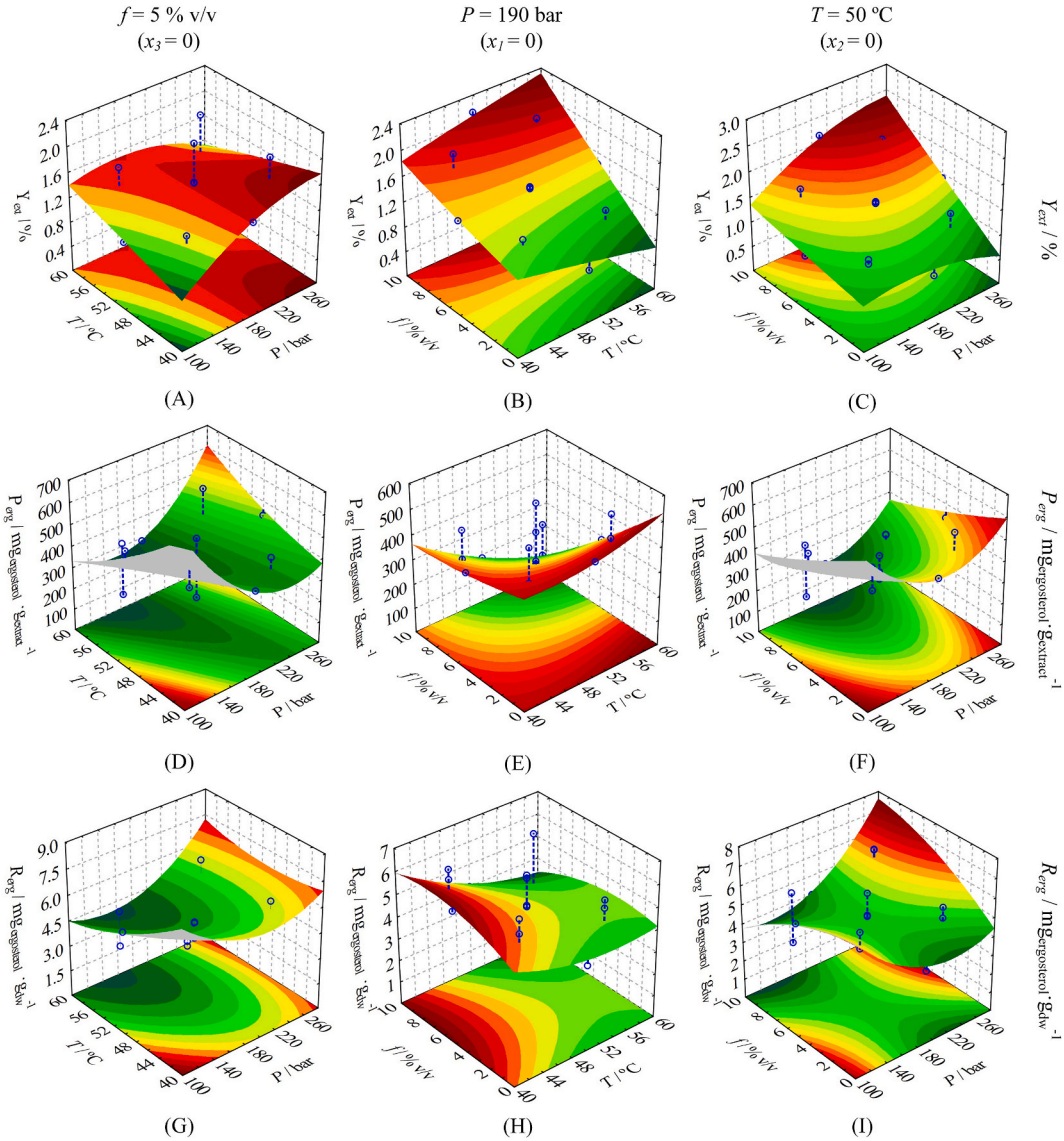

Fig. 5. Surface contour plots showing the extraction conditions' effect on (A,B,C) the extraction yield, (D,E,F) ergosterol purity in the extract, and (G,H,I) ergosterol recovery. Plots were obtained for the factors' mid-values in the experimental domain: (A,D,G) co-solvent volume fraction of 5 % v/v, (B,E,H) pressure of 90 bar, and (C,F,I) temperature of 50 °C. Different scales are used for the same response variables (z-axis) for better perceptibility.

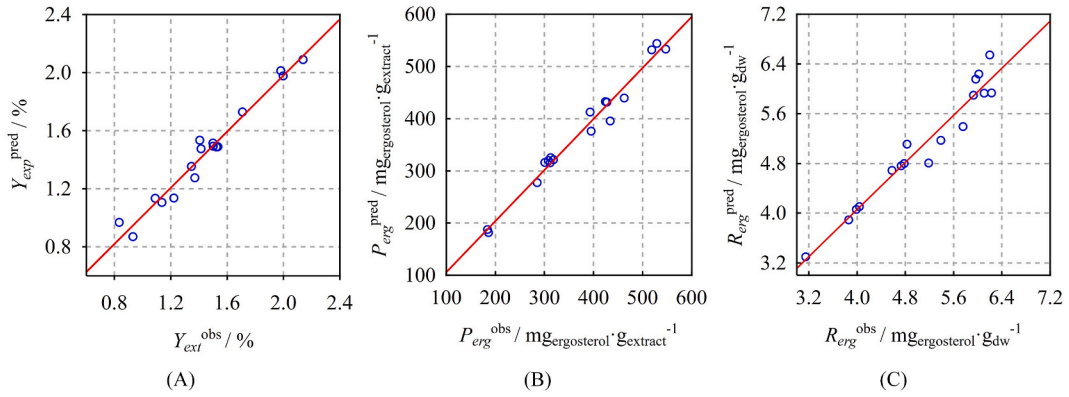

Fig. 6. Experimental versus model-predicted values for the (A) extraction yield, (B) ergosterol purity in the recovered fractions, and (C) ergosterol recovery per mushroom dry weight.

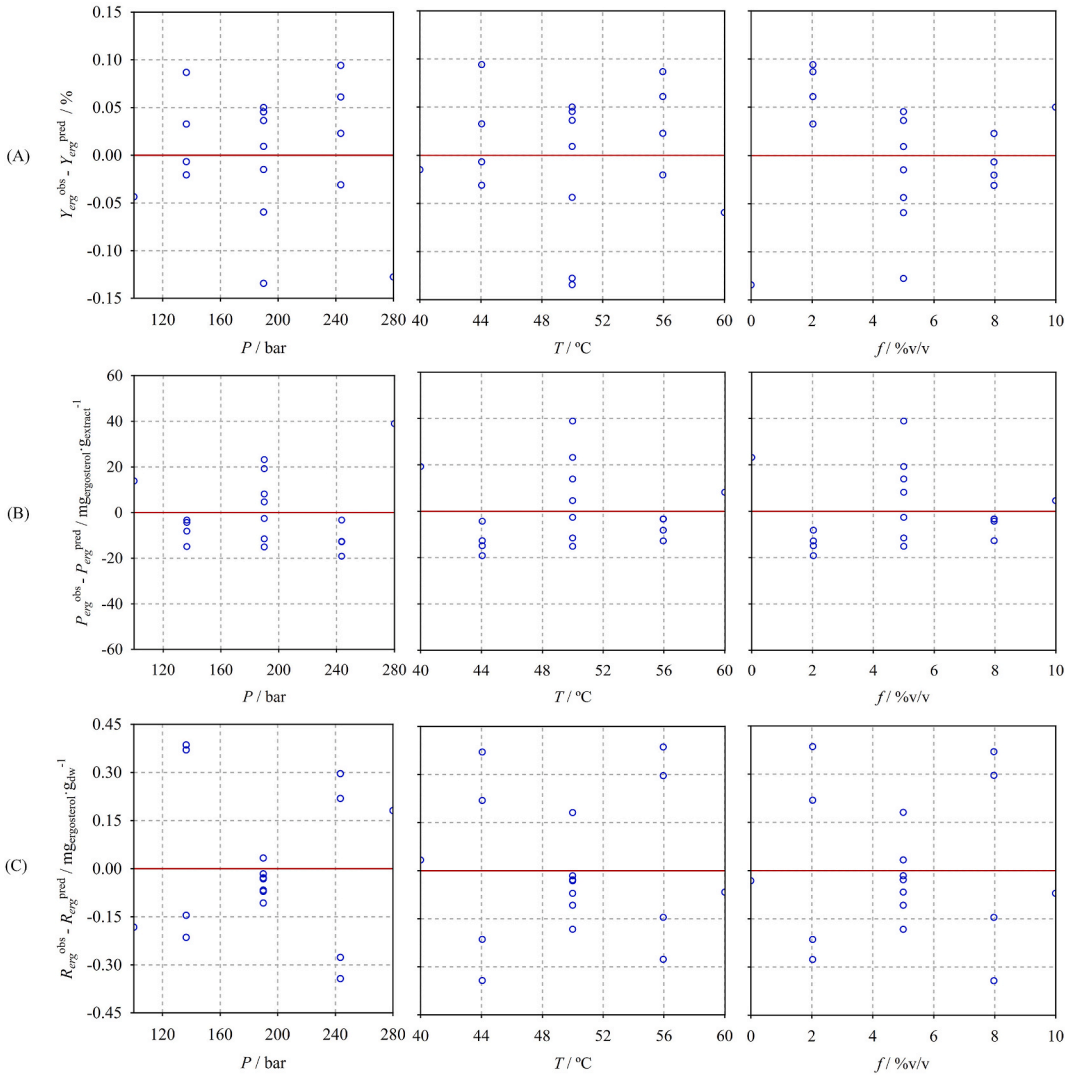

Fig. 7. Residuals' plot for the (A) extraction yield, (B) ergosterol purity in the recovered fractions and, (C) ergosterol recovery as a function of the three independent variables (pressure, temperature, and co-solvent volume percentage). Y-scale is the same in all side-by-side plots.

affect R_{erg}. Fig. 5I shows a hyperbolic paraboloid-like surface, with higher ergosterol recovery at both high *f* and *P*, and low *f* and *P* values. This plot displays a saddle point in the *Pf* plane's middle zone.

Fig. 6 displays the model-predicted responses versus their observed values (parity plots). Each blue dot represents an experimental test, and the red lines are linear regressions of the predicted response as a function of the observed value. A close agreement is observed between the experimental and the model-predicted responses. Consequently, the linear regressions between experimental and predicted responses, which are represented by red lines in Fig. 6, have a close to unity slope and a near-zero intercept. By comparing the three plots, more significant uncertainty is associated with the R_{erg} predictive model, which was expected due to **Equation (4)** and considering error propagation. This result was previously implied by this model's lower R-squared and adjusted R-squared values (see **Table 4**). Fig. 6A shows that the model's predictive capacity is more precise at higher Y_{ext}. Contrarily, Fig. 6B and C display the least accurate models' predictions for higher response values of P_{erg} and R_{erg}, respectively.

Fig. 7 presents the models' residuals, i.e., the difference between the responses' observed values and the model predictions. This figure displays nine plots, three for each response (dependent variable) as a function of the factors (independent variables). Once again, each blue dot represents an experimental test, whereas red lines indicate nill residuals. In Fig. 7, the same *y*-scale was considered in all side-by-side plots. The five levels regarding the factors' experimental domain, defined in **Table S2** (Supplementary data), are clearly identified in Fig. 7's plots. Comparing the three plots of Fig. 7A, no tendencies were identified within the residuals of the extraction yield, meaning that autocorrelations between variables were not found. Furthermore, deviations from the nill residue line (red line in all plots) displayed a similar range independently of the factor considered, further indicating unbiased results. These conclusions are also verified upon inspecting the plots of Fig. 7B and C for ergosterol extract purity and recovery, respectively. All this evidence further validates the regressed models.

4. Conclusion

In this work, ergosterol recovery from *Agaricus bisporus* mushrooms via supercritical fluid extraction was optimised using the response surface methodology with three independent variables: pressure, temperature, and co-solvent volume percentage. These variables' effects on Y_{ext}, P_{erg}, and R_{erg} was not always straightforward; thus, three predictive models, one for each response, were determined (**Equations (5)–(7)**). These models may be helpful to optimise a desired response, which may vary according to the recovered fractions' future application. Overall, it was observed that *f* was the prevalent factor, with increasing values resulting in higher Y_{ext} and lower P_{erg}; its influence on R_{erg} was not direct. Likewise, the effects of temperature and pressure on Y_{ext}, P_{erg}, and R_{erg} were complex, demanding an in-depth analysis. The maximum ergosterol purity in the recovered fractions was $(547.27 \pm 2.37)\ mg_{ergosterol} \cdot g_{extract}^{-1}$, obtained at a pressure of 100 bar, a temperature of 50 °C and 5 % v/v of co-solvent. Under these conditions, Y_{ext} and R_{erg} were 1.090 % and $(5.97 \pm 0.03)\ mg_{ergosterol} \cdot g_{dw}^{-1}$, respectively. The highest ergosterol recovery was $(6.23 \pm 0.06)\ mg_{ergosterol} \cdot g_{dw}^{-1}$, for 244 bar, 56 °C, and 8 % v/v co-solvent. In this particular case, Y_{ext} and P_{erg} were 1.999 % and $(311.80 \pm 2.96)\ mg_{ergosterol} \cdot g_{extract}^{-1}$, that is, a higher extraction yield is attained at the lower ergosterol extract purity compromise. Squared correlation coefficients close to one were obtained for all models, indicative of good-quality prediction of experimental data. Residual analysis showed a random distribution around zero, further validating the models.

Data availability statement

Data will be made available on request.

Ethics declarations

- Review or approval by an ethics committee was not needed for this study because no data of patients or experimental animals were used.
- Informed consent was not required for this study because no clinical data was used.

CRediT authorship contribution statement

Cláudia F. Almeida: Writing – original draft, Visualization, Methodology, Investigation, Formal analysis, Data curation, Conceptualization. **Yaidelin A. Manrique:** Writing – review & editing, Supervision, Conceptualization. **José Carlos B. Lopes:** Funding acquisition, Conceptualization. **Fernando G. Martins:** Writing – review & editing, Supervision. **Madalena M. Dias:** Writing – review & editing, Supervision, Project administration, Funding acquisition, Conceptualization.

Declaration of competing interest

The authors declare that they have no known competing financial interests or personal relationships that could have appeared to influence the work reported in this paper.

Acknowledgements

This work was financially supported by: Project Valor Natural (NORTE-01-0247-FEDER-024479), funded by Norte Portugal Regional Operational Programme (NORTE 2020), under the PORTUGAL 2020 Partnership Agreement, through the European Regional Development Fund (ERDF); UIDB/50020/2020 and UIDP/50020/2020 (LSRE-LCM), UIDB/00511/2020 and UIDP/00511/2020 (LEPABE), and LA/P/0045/2020 (ALiCE) funded by national funds through FCT/MCTES (PIDDAC). Cláudia Almeida acknowledges her PhD scholarship by FCT (grant number 2020.04470.BD).

Appendix A. Supplementary data

Supplementary data to this article can be found online at https://doi.org/10.1016/j.heliyon.2023.e21943.

List of abbreviations & Acronyms

ACN	Anthocyanins
BPR	Back Pressure Regulator
BSA	Bovine Serum Albumin
C3GE	Cyanidin-3-glucoside Equivalents
CCD	Central Composite Design
COSE	Conventional Organic Solvent Extraction
CP	Central Point
DW	Dry Weight
DoE	Design of Experiments
EFSA	European Food Safety Authority
FAA	Free Amino Acid
GAE	Gallic Acid Equivalent
Glu	Glucose
IS	Internal Standard
MAE	Microwave-Assisted Extraction
MIC	Minimum Inhibitory Concentration
N.D.	Not determined
N.S.	Non-significant
PE	Pyrocatechol Equivalents
PEF	Pulsed Electric Field
PLE	Pressurised Liquid Extraction
QE	Quercetin Equivalents
RSM	Response Surface Methodology
SD	Standard Deviation
SFE	Supercritical Fluid Extraction
SFE-CO_2	Supercritical Fluid Extraction with Carbon Dioxide
TPC	Total Phenolic Content
UAE	Ultrasound-Assisted Extraction
UV	Ultraviolet

References

[1] P.A. Diamantopoulou, A.N. Philippoussis, Cultivated Mushrooms: preservation and processing, in: Y.H. Hui, E.Ö. Evranuz (Eds.), Handbook of Vegetable Preservation and Processing, CRC Press, 2015, pp. 495–526.

[2] Fortunate Business Insights, Mushroom Market Size, Share & COVID-19 Impact Analysis, by Type (Button, Shiitake, Oyster, and Others), by Form (Fresh, Frozen, Dried and Canned), and Regional Forecast 2021 - 2028, 2022. Access date: April 2022. Available from: https://www.fortunebusinessinsights.com/industryreports/mushroom-market-100197.

[3] W.T. Chou, I.C. Sheih, T.J. Fang, The applications of polysaccharides from various mushroom wastes as prebiotics in different systems, J. Food Sci. 78 (7) (2013) M1041–M1048.

[4] E. Roselló-Soto, O. Parniakov, Q. Deng, A. Patras, M. Koubaa, N. Grimi, N. Boussetta, B.K. Tiwari, E. Vorobiev, N. Lebovka, F.J. Barba, Application of non-conventional extraction Methods: toward a sustainable and green production of valuable compounds from Mushrooms, Food Eng. Rev. 8 (2) (2016) 214–234.

[5] M. Ramos, N. Burgos, A. Barnard, G. Evans, J. Preece, M. Graz, A.C. Ruthes, A. Jimenez-Quero, A. Martinez-Abad, F. Vilaplana, L.P. Ngoc, A. Brouwer, B. van der Burg, M. Del Carmen Garrigos, A. Jimenez, Agaricus bisporus and its by-products as a source of valuable extracts and bioactive compounds, Food Chem. 292 (2019) 176–187.

[6] M. Blumfield, K. Abbott, E. Duve, T. Cassettari, S. Marshall, F. Fayet-Moore, Examining the health effects and bioactive components in Agaricus bisporus mushrooms: a scoping review, JNB (J. Nutr. Biochem.) 84 (2020), 108453.

[7] Y. Feng, J. Zhang, C. Wen, C. Sedem Dzah, I. Chidimma Juliet, Y. Duan, H. Zhang, Recent advances in Agaricus bisporus polysaccharides: extraction, purification, physicochemical characterization and bioactivities, Process Biochemistry 94 (2020) 39–50.

[8] Y.K. Leong, F.C. Yang, J.S. Chang, Extraction of polysaccharides from edible mushrooms: emerging technologies and recent advances, Carbohydrate Polymers 251 (2021), 117006.
[9] L. López-Hortas, N. Flórez-Fernández, M.D. Torres, H. Domínguez, Update on potential of edible mushrooms: high-value compounds, extraction strategies and bioactive properties, International Journal of Food Science & Technology 57 (3) (2022) 1378–1385.
[10] I. Ahmad, M. Arif, M.M. Xu, J.Y. Zhang, Y.T. Ding, F. Lyu, Therapeutic values and nutraceutical properties of shiitake mushroom (Lentinula edodes): a review, Trends Food Sci. Technol. 134 (2023) 123–135.
[11] G. Lin, Y. Li, X. Chen, F. Zhang, R.J. Linhardt, A. Zhang, Extraction, structure and bioactivities of polysaccharides from Sanghuangporus spp.: a review, Food Biosci. (2023) 53.
[12] Y. Shevchuk, K. Kuypers, G.E. Janssens, Fungi as a source of bioactive molecules for the development of longevity medicines, Ageing Res. Rev. 87 (2023), 101929.
[13] J.C.M. Barreira, M.B.P.P. Oliveira, I.C.F.R. Ferreira, Development of a Novel Methodology for the analysis of ergosterol in Mushrooms, Food Anal. Methods 7 (1) (2013) 217–223.
[14] S.A. Heleno, P. Diz, M.A. Prieto, L. Barros, A. Rodrigues, M.F. Barreiro, I.C. Ferreira, Optimization of ultrasound-assisted extraction to obtain mycosterols from Agaricus bisporus L. by response surface methodology and comparison with conventional Soxhlet extraction, Food Chem. 197 (2016) 1054–1063. Pt B.
[15] S.H. Hu, Z.C. Liang, Y.C. Chia, J.L. Lien, K.S. Chen, M.Y. Lee, J.C. Wang, Antihyperlipidemic and antioxidant effects of extracts from Pleurotus citrinopileatus, J. Agric. Food Chem. 54 (6) (2006) 2103–2110.
[16] A. Villares, A. García-Lafuente, E. Guillamón, Á. Ramos, Identification and quantification of ergosterol and phenolic compounds occurring in Tuber spp. truffles, J. Food Compos. Anal. 26 (1–2) (2012) 177–182.
[17] J.H. Kang, J.E. Jang, S.K. Mishra, H.J. Lee, C.W. Nho, D. Shin, M. Jin, M.K. Kim, C. Choi, S.H. Oh, Ergosterol peroxide from Chaga mushroom (Inonotus obliquus) exhibits anti-cancer activity by down-regulation of the beta-catenin pathway in colorectal cancer, J. Ethnopharmacol. 173 (2015) 303–312.
[18] O. Taofiq, S.A. Heleno, R.C. Calhelha, I.P. Fernandes, M.J. Alves, L. Barros, A.M. González-Paramás, I.C.F.R. Ferreira, M.F. Barreiro, Phenolic acids, cinnamic acid, and ergosterol as cosmeceutical ingredients: stabilization by microencapsulation to ensure sustained bioactivity, Microchem. J. 147 (2019) 469–477.
[19] A. Gil-Ramirez, A. Ruiz-Rodriguez, F.R. Marin, G. Reglero, C. Soler-Rivas, Effect of ergosterol-enriched extracts obtained from Agaricus bisporus on cholesterol absorption using an in vitro digestion model, J. Funct.Foods 11 (2014) 589–597.
[20] W.-S. He, D. Cui, L. Li, J. Rui, L.-T. Tong, Plasma triacylglycerol-reducing activity of ergosterol linolenate is associated with inhibition of intestinal lipid absorption, J. Funct.Foods 64 (2020) 103686.
[21] S.A. Heleno, M.A. Prieto, L. Barros, A. Rodrigues, M.F. Barreiro, I.C.F.R. Ferreira, Optimization of microwave-assisted extraction of ergosterol from Agaricus bisporus L. by-products using response surface methodology, Food Bioprod. Process. 100 (2016) 25–35.
[22] J.-L. Bresson, B. Burlingame, Dean, T. Fairweather-Tait, S. Heinonen, M. Hirsch-Ernst, K.-I. Mangelsdorf, I. Mcardle, H. Naska, A. Neuhäuser-Berthold, M. Nowicka, G. Pentieva, K. Sanz, Y. S, A. S, A. S, M, D. Tomé, D. Turck, H.V. Loveren, M. Vinceti, P. Willatts, C. Lamberg-Allardt, H. Przyrembel, I. Tetens, Scientific Opinion on Dietary Reference Values for Vitamin D, vol. 179, European Food Safety Authority Journal, 2016.
[23] E. Shaikh, L. Khare, R. Jain, P. Dandekar, Design of experimental approach for maximal extraction of vitamin D_2 from mushrooms, J. Food Nutr. Res. 59 (4) (2020) 367–379.
[24] F.K. Nzekoue, Y. Sun, G. Caprioli, S. Vittori, G. Sagratini, Effect of the ultrasound-assisted extraction parameters on the determination of ergosterol and vitamin D_2 in Agaricus bisporus, A. bisporus Portobello, and Pleurotus ostreatus mushrooms, J. Food Compos. Anal. 109 (2022).
[25] P. Mattila, A.-M. Lampi, R. Ronkainen, J. Toivo, V. Piironen, Sterol and vitamin D_2 contents in some wild and cultivated mushrooms, Food Chem. 76 (3) (2002) 293–298.
[26] SkyQuest, Global Mushroom Market size, share growth analysis, by type (button Mushroom, shiitake Mushroom), By Form (Fresh Mushroom, Frozen Mushroom) - Industry Forecast 2023-2030, 2023. Access date: April 2023. Available from: https://www.skyquestt.com/report/mushroom-market.
[27] M. Rühl, U. Kües, Mushroom production, in: U. Kües (Ed.), Wood Production, Wood Technology, and Biotechnological Impacts, Universitätsverlag Göttingen, 2007, pp. 555–586.
[28] A.N. Philippoussis, Production of Mushrooms using agro-industrial residues as substrates, in: Biotechnology for Agro-Industrial Residues Utilisation, 2009, pp. 163–196.
[29] E.M.C. Alexandre, S.A. Moreira, L.M.G. Castro, M. Pintado, J.A. Saraiva, Emerging technologies to extract high added value compounds from fruit residues: sub/supercritical, ultrasound-, and enzyme-assisted extractions, Food Rev. Int. 34 (6) (2017) 581–612.
[30] C.M. Galanakis, Recovery of high added-value components from food wastes: conventional, emerging technologies and commercialized applications, Trends Food Sci. Technol. 26 (2) (2012) 68–87.
[31] S. Saha, A.K. Singh, A.K. Keshari, V. Raj, A. Rai, S. Maity, Modern extraction techniques for drugs and medicinal agents, in: A.M. Grumezescu, A.M. Holban (Eds.), Ingredients Extraction by Physicochemical Methods in Food, Andre Gerhard Wolff, United Kingdom, 2017.
[32] M.K.L. Bicking, Analytical extractions, in: I.D. Wilson (Ed.), Encyclopedia of Separation Science, Academic Press, 2000, pp. 1371–1382.
[33] J.M. Prado, R. Vardanega, I.C.N. Debien, M.A.d.A. Meireles, L.N. Gerschenson, H.B. Sowbhagya, S. Chemat, Conventional extraction, in: Food Waste Recovery, 2015, pp. 127–148.
[34] A. Gil-Ramírez, L. Aldars-García, M. Palanisamy, R.M. Jiverdeanu, A. Ruiz-Rodríguez, F.R. Marín, G. Reglero, C. Soler-Rivas, Sterol enriched fractions obtained from Agaricus bisporus fruiting bodies and by-products by compressed fluid technologies (PLE and SFE), Innovat. Food Sci. Emerg. Technol. 18 (2013) 101–107.
[35] G. Sodeifian, N. Saadati Ardestani, S.A. Sajadian, Extraction of seed oil from Diospyros lotus optimized using response surface methodology, J. For. Res. 30 (2) (2018) 709–719.
[36] J.A. Mendiola, M. Herrero, M. Castro-Puyana, E. Ibáñez, Supercritical fluid extraction, in: Natural Product Extraction - Principles and Applications, The Royal Society of Chemistry Publishing, United Kingdom, 2013, pp. 196–230.
[37] G.N. Sapkale, S.M. Patil, U.S. Surwase, P.K. Bhatbhage, Supercritical fluid extraction, International Journal of Chemical Science 8 (2) (2010) 729–743.
[38] L. Barros, T. Cruz, P. Baptista, L.M. Estevinho, I.C. Ferreira, Wild and commercial mushrooms as source of nutrients and nutraceuticals, Food Chem. Toxicol. 46 (8) (2008) 2742–2747.
[39] A.S. Bengu, The fatty acid composition in some economic and wild edible mushrooms in Turkey, Prog. Nutr. 22 (1) (2020) 185–192.